INSTITUTE OF PHYSICS PUBLISHING JOURNAL OF PHYSICS D: APPLIED PHYSICS

J. Phys. D: Appl. Phys. **37** (2004) 1841–1844 PII: S0022-3727(04)77294-0

# Vacancy defects in epitaxial $La_{0.7}Sr_{0.3}MnO_3$ thin films probed by a slow positron beam

**S W Jin[1,4], X Y Zhou[1,2], W B Wu[2], C F Zhu[3], H M Weng[1], H Y Wang[1], X F Zhang[1], B J Ye[1] and R D Han[1]**

[1] Department of Modern Physics, University of Science and Technology of China, PO Box 4, Hefei 230026, People's Republic of China

[2] Structure Research Laboratory, University of Science and Technology of China, Hefei 230026, People's Republic of China

[3] Department of Materials Science and Engineering, University of Science and Technology of China, Hefei 230026, People's Republic of China

E-mail: jinsw@mail.ustc.edu.cn

Received 6 March 2004
Published 16 June 2004
Online at stacks.iop.org/JPhysD/37/1841
doi:10.1088/0022-3727/37/13/017

**Abstract**

Vacancy defects in epitaxial $La_{0.7}Sr_{0.3}MnO_3$ (LSMO) thin films on $LaAlO_3$ substrates were detected using a variable energy positron beam. The line-shape $S$ parameter of the epitaxial thin films deposited at different oxygen pressures was measured as a function of the implanting positron energy $E$. Our results show that the $S$ parameter of the films changes non-monotonically with their deposition oxygen pressures. For the films deposited at lower oxygen pressures, the increase in $S$ value in the films is attributed to the increase in oxygen vacancies and/or related defect–$V_O$ complexes, and for those deposited at higher oxygen pressures, the larger $S$ parameter of the films is caused by the grain boundaries and/or metallic ion vacancies. The surface morphology of the films was also characterized to analyse the open volume defects in the LSMO films.

## 1. Introduction

The discovery of colossal magnetoresistance in $La_{1-x}A_xMnO_3$ (A = Ba, Sr, Ca) thin films has renewed interest in these manganese oxides [1–3]. The physical properties of these hole-doped compounds depend dramatically on the doping level, and the phase diagram of these compounds for various states, such as ferromagnetic conducting, antiferromagnetic insulating, ferromagnetic insulating, charge ordering, orbital ordering, etc [4] has been established. $La_{1-x}Sr_xMnO_3$, which is one kind of manganese oxide, has a perovskite crystal structure [5] and is lattice-matched with the other perovskites such as $Pb(Zr,Ti)O_3$. Recently, $La_{0.7}Sr_{0.3}MnO_3$ (LSMO) thin films have been used as electrodes for highly oriented ferroelectric thin film capacitors [6–8]. These authors suggested that the oxygen vacancies and related defect–dipole complexes in both LSMO and the $Pb(Zr_{0.52},Ti_{0.48})O_3$ layers caused fatigue and imprint of the ferroelectric capacitors. Therefore, studies on the vacancy-related defects in these metal-oxide films are of great importance.

Positron annihilation spectroscopy (PAS) is an important method to detect vacancy defects, from single atom vacancies to large voids [9]. A variable energy positron beam with an adjustable energy and a narrow energy distribution allows depth-resolved measurement, and can be applied to defect studies of thin films. When a positron is implanted into condensed matter, it annihilates with an electron and emits two 511 keV $\gamma$ quanta [10]. The energy spectrum is Doppler broadened by the finite momentum of the annihilating pair, which is dominated by that of the electron. This spectrum was characterized by a line-shape $S$ parameter. An increase in positrons trapping to vacancy-related defects results in a narrowing of the spectrum, and increases the $S$ parameter. The same occurs if the size of the open volume of the positron trapping defects increases.

[4] Author to whom any correspondence should be addressed.

  

In this paper the line-shape $S$ parameter of the positron annihilation spectrum as a function of the implanting positron energy was measured for epitaxial LSMO thin films deposited at different oxygen pressures and on $LaAlO_3$ (LAO) substrates. A defect model based on the Kröger–Vink notation [11] was used to identify the defect types in the LSMO films. The surface morphology was measured to analyse the open volume of defects in the LSMO films.

## 2. Experimental details

Epitaxial $La_{0.7}Sr_{0.3}MnO_3$ thin films were deposited on a single-crystal substrate $LaAlO_3$ (001) by using the pulsed-laser deposition method. An excimer KrF laser ($\lambda = 248$ nm) with a repetition rate of 10 Hz was used to ablate a stoichiometric $La_{0.7}Sr_{0.3}MnO_3$ target. Before deposition, the chamber was evacuated by a cryopump to a base pressure of $5 \times 10^{-7}$ Torr. For the LSMO thin films, the deposition temperature and *in situ* annealing temperature were fixed at 680 °C, whereas the deposition oxygen pressures were set at 125 mTorr, 60 mTorr and 35 mTorr, respectively. As-grown films were annealed and cooled in the same oxygen ambient as during deposition. The thickness of the LSMO films is about 200 nm. The phase and crystallinity of the LSMO films were characterized by x-ray diffraction (XRD) ($\theta$–$2\theta$ scan and $\omega$-scan rocking curves) using Cu K$\alpha$ ($\lambda = 1.541$ Å) radiation. Results show that only the $(00l, l = 1, 2, \ldots,)$ diffraction lines of the phase were observed, and the sample was grown epitaxially with the $c$-axis normal to the substrate surface. The surface morphology was measured using scanning electron microscopy (SEM) for these films.

A variable energy positron beam [12] was used to study the defect depth profile of the LSMO/LAO samples. The annihilation quanta were measured using a high purity Ge detector with a resolution of 1.2 keV (FWHM) at 514 keV $\gamma$-rays of $^{85}$Sr. About $5 \times 10^5$ total counts were accumulated in each spectrum. The Doppler broadening of the annihilation radiation was analysed in terms of the line-shape $S$ parameter, defined as the ratio of the integral over a fixed central portion of the peak ($A$, 510–512 keV) to the total counts ($B$, 503–518 keV), according to $S = A/B$ (which yields a value of ~0.500 for defect-free silicon). The relationship between the observed $S$ and $E$ was analysed using VEPFIT, a computer program developed by van Veen *et al* [13]. In this procedure, the region sampled by positrons was divided into several blocks. Under these conditions, VEPFIT was used to determine the fraction of positrons annihilated in each block and the corresponding $S$ parameter. The observed $S$–$E$ relationships were fitted to the following equation:

$$S(E) = S_S F_S(E) + \sum S_i F_i(E), \qquad (1)$$

where $F_S(E)$ is the fraction of positrons annihilated at the surface, $F_i(E)$ is that in the $i$th block ($F_S(E) + \Sigma F_i(E) = 1$), and $S_S$ and $S_i$ are the $S$ parameters for the annihilation of positrons at the surface and in the $i$th block, respectively.

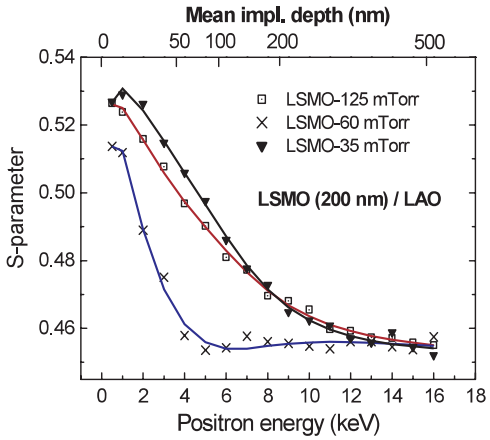


**Figure 1.** The $S$ parameter as a function of the implanting positron energy for the LSMO/LAO samples, the solid curves are fitted results from equation (1).

## 3. Results and discussion

### *3.1. Variation of the S parameter with the implanting positron energy E*

Figure 1 shows the $S$ parameter of the LSMO/LAO samples as a function of the implanting positron energy $E$. In the figure, the mean implantation depth [13] of positrons is shown at the upper horizontal axis. The observed $S$ parameter displays a common feature as a function of incident energy, i.e. the $S$ parameter of the samples decreases monotonically with increasing positron energy $E$. When the energy $E < 9$ keV the positrons are implanted into the LSMO film layer (corresponding depth 200 nm), and when $E > 9$ keV some of the positrons are implanted into the LAO substrate (since the energy width of the implantation profile (FWHM) scales with the implantation energy).

The variation of the line-shape $S$ parameter with the incident energy $E$ can be understood qualitatively [14]. Because of the positron surface states and trapping at the surface defects, the $S$ at the surface ($E \cong 0$ keV) is larger than that within the LSMO film and the single-crystal substrate. The epitaxial thin film contains many crystalline imperfections, some of which can trap positrons, so the $S$ parameter of the film layer (corresponding implanted energy $E < 9$ keV) is larger than that of the single-crystal substrate. When the energy $E > 9$ keV some of the positrons penetrate into the substrate, and because of the implanting profile and back diffusion of positrons, some of the positrons that are implanted into the substrate could diffuse back to the subsurface region (9 keV $< E <$ 13 keV) and annihilate at the subsurface. This is the reason why the $S$ parameter decreases slowly down to annihilation characteristics in the substrate. $S$ approaches a constant at high energies $E > 13$ keV, which indicates that positrons implant into the substrate bulk and annihilate in the bulk without diffusing back to the thin film region. In figure 1, we see that the $S$ parameter of the LSMO layer grown at 35 mTorr is slightly larger than that of the LSMO layer grown at 125 mTorr, and the $S$ parameter of the LSMO layer grown at 60 mTorr is the least for the three samples. For the films deposited at 60 mTorr, however, when the energy $E > 6$ keV

**Table 1.** The diffusion length $L_{\text{eff}}$ of positrons for the LSMO layer, and characteristic $S$ values corresponding to the LSMO layer and substrate.

| Sample | $L_{\text{eff}}$ (nm) | $S_{\text{LSMO}}$ | $S_{\text{Sub}}$ |
|---|---|---|---|
| LSMO-125 mTorr | $48.7 \pm 1.9$ | $0.4785 \pm 0.0014$ | $0.4514 \pm 0.0018$ |
| LSMO-60 mTorr | $21.4 \pm 0.6$ | $0.4475 \pm 0.0011$ | $0.4513 \pm 0.0019$ |
| LSMO-35 mTorr | $71.6 \pm 3.9$ | $0.4828 \pm 0.0026$ | $0.4523 \pm 0.0018$ |

the $S$ parameter approaches an annihilation characteristic in the substrate; the details will be discussed in section 3.2.

### *3.2. Variation of the S parameter with deposition oxygen pressure*

For the three LSMO/LAO samples, the observed $S$–$E$ curves were fitted to equation (1), and the distribution of $S$ was assumed to be homogeneous for the LSMO layer. The fitted results are listed in table 1. The solid curves shown in figure 1 are the fitting results. The large $S_{\text{LSMO}}$ parameters and short diffusion length $L_{\text{eff}}$ values for the LSMO films can be ascribed to the positron trapping by vacancy-related defects. The typical value of $L_{\text{eff}}$ in semiconductor materials, such as Si [15] and GaAs [16], is 200–300 nm, and that in metallic Cu [17], is 150–200 nm. In this work, the values of $L_{\text{eff}}$ on the LSMO layers are smaller than the typical value of $L_{\text{eff}}$ on the defect-free materials. Therefore, the diffusion of positrons is likely to be suppressed by the trapping or scattering of defects within LSMO layers. In the fitting procedure, the region sampled by positrons was divided into two blocks (the first block corresponds to the film layer and the second corresponds to the LAO substrate); the value of the diffusion length in the substrate is set at $230 \pm 10$ nm, and the derived values of $S_{\text{Sub}}$ do not differ for the three samples. In the following discussion, we focus on the change in the $S$ parameter of the LSMO layer (i.e. $S_{\text{LSMO}}$) with the deposition oxygen pressure.

The fitted $S$ parameter of the LSMO layer changes non-monotonically with the deposition oxygen pressures, which relates the two functions of the deposition oxygen pressure: (i) supplying deficient oxygen atoms during deposition of LSMO films, (ii) decreasing the energy of the depositing particles by colliding with ambient oxygen atoms.

From table 1, we find that the fitted $S$ value of the LSMO film deposited at 60 mTorr of oxygen pressure is 0.4475, which increases to $S_{125} = 1.069S_{60}$ for the films deposited at 125 mTorr. This increase of $S$ could be explained qualitatively. At higher oxygen pressures, the ablated particles will lose more energy after colliding with ambient oxygen atoms. Furthermore, at higher oxygen pressures, more oxygen atoms will be trapped at the substrate surface, and after the ablated species arrive at the substrate, they will have to expend some energy to kick off the trapped oxygen atoms. These factors will result in an increase in the vacancy defects in the LSMO films deposited at 125 mTorr. For the LSMO film deposited at 35 mTorr, however, the $S$ parameter of the film increases to $S_{35} = 1.079S_{60}$. The lower oxygen pressure causes oxygen deficiency during the deposition, leaving more oxygen vacancies, $V_O$, or defect–$V_O$ complexes in the film grown at 35 mTorr, which also results in the increase in the $S$ parameter. The lower value of $S$ in the film deposited at 60 mTorr can be attributed to the lower defect concentration that resulted from the competition between the two functions of the deposition oxygen pressures. Previously, Zhou *et al* [18] reported that the concentration of the defects increases with increase in air partial pressures on an epitaxial $YBa_2Cu_3O_{7-x}$ film. Here, we observed that the concentration of the defects increases both with the increase in oxygen pressure and with the reduction in oxygen. This implies that there is an optimum oxygen pressure, which induces a high crystalline quality in the grown films.

From figure 1 and table 1, the steep $S$ parameter profile and short diffusion length ($L_{\text{eff}} \approx 22$ nm) of the LSMO film grown at 60 mTorr cannot only be ascribed to the higher crystalline quality, but could be related to the local structure of the Mn–$O_6$ octahedron, which may scatter the positrons. Therefore, further studies on the local charge distribution of the Mn–$O_6$ octahedron or of the oxygen dynamics of the deposition films need to be performed.

### *3.3. Identification of the vacancy defects in LSMO films*

In a previous study, Wu *et al* [7] reported that the $La_{0.7}Sr_{0.3}MnO_3$ films grown at 620°C and 400–75 mTorr of oxygen tend to be oxygen stoichiometric, and the films deposited at 75–10 mTorr tend to be under oxygen stoichiometric. Thus, the vacancy defects of the LSMO films deposited at 125 mTorr are different from that of the films deposited at 35 and 60 mTorr. A defect model based on the Kröger–Vink [11] notation was used to identify the defect types in the LSMO films. In stoichiometric $LaMnO_3$, the charge states of La and Mn ions can both be expected to be 3+. When $Sr^{2+}$ ions replace $La^{3+}$ ions, to compensate for this charge difference, the $Mn^{3+}$ ions change to $Mn^{4+}$ ions, as shown in the following Sr doping reaction (using Kröger–Vink notation):

$$\text{SrO} + \tfrac{1}{4}\text{O}_2 + (\text{La}^{3+}{}_{\text{La}^{3+}})^x + (\text{Mn}^{3+}{}_{\text{Mn}^{3+}})^x = \tfrac{1}{2}\text{La}_2\text{O}_3 + (\text{Sr}^{2+}{}_{\text{La}^{3+}})' + (\text{Mn}^{4+}{}_{\text{Mn}^{3+}})^{\bullet}, \quad (2)$$

where the $(\text{Mn}^{4+}{}_{\text{Mn}^{3+}})^{\bullet}$ species can be thought of as holes which are responsible for the higher electrical conductivity of the manganese oxides [7, 8, 19]. When the doping $x$ of Sr is fixed, the number of $(\text{Mn}^{4+}{}_{\text{Mn}^{3+}})^{\bullet}$ also depends on the oxygen content of the films. The LSMO films deposited at the understoichiometric oxygen pressure [7] (i.e. 75–10 mTorr), loses oxygen according to the following reaction:

$$2(\text{Mn}^{4+}{}_{\text{Mn}^{3+}})^{\bullet} + (\text{O}^{2-}{}_{\text{O}^{2-}})^x = \tfrac{1}{2}\text{O}_2 + 2(\text{Mn}^{3+}{}_{\text{Mn}^{3+}})^x + (\text{V}_{\text{O}^{2-}})^{\bullet\bullet}. \quad (3)$$

Equation (3) shows that when one oxygen vacancy forms, two holes ($(\text{Mn}^{4+}{}_{\text{Mn}^{3+}})^{\bullet}$) are consumed. So, the oxygen vacancies ($(\text{V}_{\text{O}^{2-}})^{\bullet\bullet}$) are majority defects of the LSMO films deposited at 35 and 60 mTorr, and the larger $S$ value of the films deposited at 35 mTorr is caused by the increase in the oxygen vacancies and/or related-defect complexes. According to a simple ionic model the local charge state of $V_O$ should be 2+; however, the association of the oxygen vacancy, $V_O$, and two neighbouring $Sr^{2+}$ ions can trap positrons.

From equation (3), the oxygen vacancies and/or related-defect complexes cannot be majority defects for the LSMO films deposited at stoichiometric oxygen pressure. To find the cause of the larger $S$ of the film grown at 125 mTorr, the surface morphology of the LSMO films has been measured.

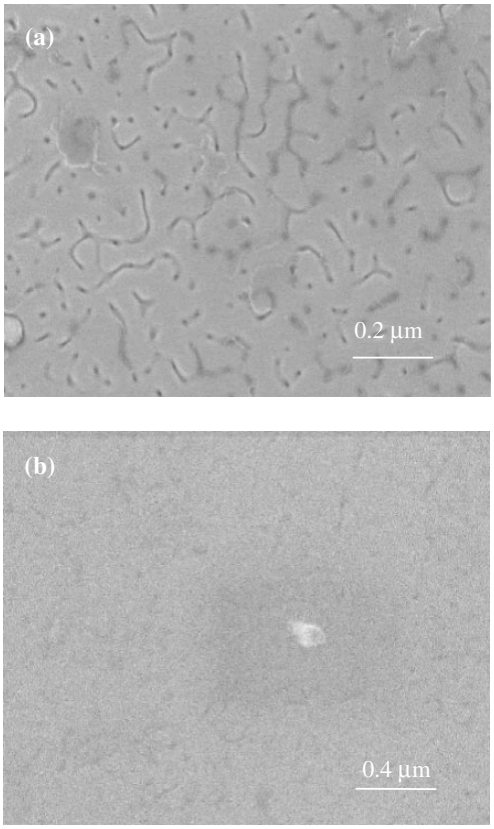


**Figure 2.** SEM pictures of the LSMO films grown at 125 mTorr (*a*) and 60 mTorr (*b*), respectively.

Figure 2 shows the SEM images of the LSMO films grown at 125 mTorr and 60 mTorr, respectively (the image of the films deposited at 35 mTorr is similar to that of the films grown at 60 mTorr). It is seen that the surface morphology of the films improves dramatically at lower oxygen pressures. In [20], we have reported that the LSMO film of 125 mTorr has a lower crystallinity based on the XRD $\omega$-scan rocking curves. From the surface morphology and $\omega$-scan rocking curves, we see that the grain (or column) boundaries and/or lower crystallinity should be responsible for the larger $S$ of the films deposited at 125 mTorr. The lattice strain at the LSMO layer/substrate interface and the defects associated with it may also have an effect on the positron spectra; this will examined in further studies.

Friessnegg *et al* [21] reported that metallic ion vacancies (situated in the La sublattice) and oxygen vacancies exist in the film $La_{1-x}Sr_xCoO_3$ (LSCO). Here, we suggest that the metallic ion vacancies (such as $V_{La}$) and oxygen vacancies can also induce the increase in $S$ in the LSMO films deposited at 125 mTorr. This is due to the lattice structure of the LSCO being similar to that of the LSMO; the deposition condition of these oxide films is similar too.

## 4. Conclusions

In summary, vacancy-related defects in epitaxial LSMO thin films on $LaAlO_3$ substrates were detected using a variable energy positron beam. A defect model based on the Kröger–Vink notation and the surface morphology were used to identify the defect types of the LSMO films deposited at different oxygen pressures. The results show that the oxygen vacancies ($(V_{O^{2+}})^{\bullet\bullet}$) are majority defects of the LSMO films deposited at 35 and 60 mTorr. For the LSMO films deposited at lower oxygen pressures (such as 35 mTorr), the increase of $S$ in the films is attributed to the increase in oxygen vacancies ($(V_{O^{2+}})^{\bullet\bullet}$) and/or related defect-$(V_{O^{2+}})^{\bullet\bullet}$ complexes. For the LSMO films deposited at 125 mTorr, however, the larger $S$ parameter of the films is caused by the grain (or column) boundaries and/or metallic ion vacancies.

## Acknowledgments

This work was supported by the National Natural Science Foundation of China under grant nos 10175061 and 10075044.

## References

[1] von Helmol R, Wecker J, Holzapfel B, Schultz L and Samwer K 1993 *Phys. Rev. Lett.* **71** 2331
[2] Chahara S, Ohno T, Kasai K and Kozono Y 1993 *Appl. Phys. Lett.* **63** 1990
[3] Jin S, Tiefel T H, McCormack M, Fastnacht R A, Ramesh R and Chen L H 1994 *Science* **264** 413
[4] Schiffer P, Ramirez A P, Bao W and Cheong S W 1995 *Phys. Rev. Lett.* **75** 3336
[5] Hemberger J, Krimmel A, Kurz T, Krug von Nidda H-A, Ivanov V Yu, Mukhin A A, Balbashov A M and Loidl A 2002 *Phys. Rev.* B **66** 094410
[6] Wu W B, Wong K H, Choy C L and Zhang Y H 2000 *Appl. Phys. Lett.* **77** 3441
[7] Wu W B, Wong K H, Mak C L, Choy C L and Zhang Y H 2000 *J. Vac. Sci. Technol.* A **18** 2412
[8] Wu W B, Wong K H, Choy C L and Zhang Y H 2001 *Thin Solid Films* **389** 56
[9] Triftshäuser W 1986 *Microscopic Methods in Metals* ed U Gonser (Berlin: Springer) p 249
[10] Krause-Rehberg R and Leipner H S 1999 *Positron Annihilation in Semiconductors* (*Solid-State Sciences* vol 127) (Berlin: Springer)
[11] Kröger F A and Vink H J 1957 *Solid State Physics Advances in Research and Applications* vol 3, ed F Seitz and T Turnbull (New York: Academic) p 307
[12] Han R D *et al* 1988 *Acta Phys. Sin.* **37** 1517
[13] van Veen A, Schut H, de Vries J, Hakvoort R A and Ijpma M R 1990 *AIP Conf. Proc.* **218** 171
[14] Kogel G 1995 *Mater. Sci. Forum.* **175–178** 107
[15] Nielsen B, Lynn K G, Welch D O, Leung T C and Rubloff G W 1989 *Phys. Rev.* B **40** 1434
[16] Uedono A, Wei L, Tabuki Y, Kondo H, Tanigawa S, Wada K and Nakanishi H 1991 *Japan. J. Appl. Phys.* part 2 **30** L2002
[17] Uedono A, Tanigawa S and Sakairi H 1991 *J. Nucl. Mater.* **184** 191
[18] Zhou X Y, Lu Xuekun, Jiang H, Bauer-Kugelmann W, Duffy J A, Kögel G and Triftshauser W 1997 *J. Phys.: Condens. Matter.* **9** L61
[19] Coey J M D, Viret M, Ranno L and Ounadjela K 1995 *Phys. Rev. Lett.* **75** 3910
[20] Jin S W *et al* 2004 *Chin. J. Low. Temp. Phys.* **26** 95
[21] Friessnegg T, Madhuker S, Nielsen B, Moodenbaugh A R, Aggarwal S, Keeble D J, Poindexter E H, Mascher P and Ramesh R 1999 *Phys. Rev.* B **59** 13365